Sequence Dependence and Direct Measurement of Crossover Isomer Distribution in Model Holliday Junctions using NMR spectroscopy†

Göran Carlström‡ and Walter J. Chazin*

Department of Molecular Biology, The Scripps Research Institute, 10666 North Torrey Pines Road, La Jolla, California 92037

Received October 30, 1995; Revised Manuscript Received January 11, 1996⊗

ABSTRACT: A 32-base-pair model of the Holliday junction (HJ) intermediate in genetic recombination has been prepared and analyzed in-depth by 2D and 3D ^{1}H NMR spectroscopy. This HJ (J2P1) corresponds to a cyclic permutation of the base pairs at the junction relative to a previously studied HJ [J2; Chen, S.-M., & Chazin, W. J. (1994) *Biochemistry 33*, 11453−11459], designed to probe the effect of the sequence at the $n - 1$ position (where n is the residue directly at the branch point) on the stacking geometry. Observation of several interbase nuclear Overhauser effects (NOEs) clearly indicates a strong preference for the isomer opposite that observed for J2, confirming the dependence of stacking isomer preference on the sequence at the junction. As for other model HJs studied, a small equilibrium distribution of the alternate isomer could be identified. A sample of J2P1 was prepared with a single ^{15}N-labeled thymine residue at the branch point. 1D ^{15}N-filtered ^{1}H-detected experiments on this sample at low temperature give strong support for the co-existence of the two stacking isomers and provide a much more direct and accurate measure of the crossover isomer distribution. The comparative analysis of our immobile HJs and a model cruciform structure [Pikkemaat, J. A., van den Elst, H., van Boom, J. H., & Altona, C. (1994) *Biochemistry 33*, 14896−14907] sheds new light on the issue of the relevance of crossover isomer preference *in vivo*.

There is a considerable interest in the study of branched DNA structures because these are postulated as intermediates in a variety of genetic processes involving DNA rearrangements. Among the most well-studied of these is the four-arm Holliday junction (HJ;[1] Holliday, 1964), a key intermediate in most DNA recombinations and many repair processes in the cell (Stahl, 1994; Kowalczykowski *et al.*, 1994). The Holliday junction (Figure 1) is formed when two DNA duplexes are cross-ligated. In homologous recombination, the importance of the HJs *in vivo* stems from their intrinsic symmetry at the point where the four arms meet; when HJs are resolved by specific enzymes (resolvases), they can either regenerate essentially the original (parental) pair of duplexes or recombine to produce the alternate (recombinant) pairing of the four duplex arms. A significant body of evidence has accumulated indicating that the outcome of HJ resolution is dependent on the DNA sequence at the branching point but that the recognition and cleavage events are not due to the sequence *per se*, but rather to the details of the high-order structure specified by a given sequence [for reviews, see Lilley and Clegg (1993a,b), and Seeman and Kallenbach (1994)]. Hence, an understanding of recombination and repair events at the molecular level requires detailed information on HJ structure and knowledge of the dependence of the structure on the nucleotide sequence.

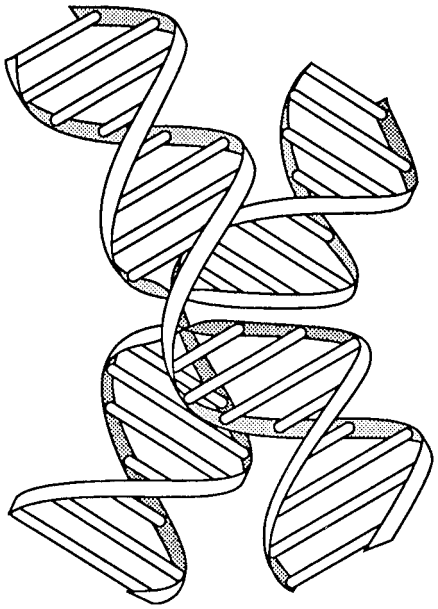

FIGURE 1: Schematic diagram of the stacked-X structure of the Holliday junction.

The studies reported here are designed to determine the sequence dependence of HJ structure, working from the basis that there are two possible ways in which the duplex arms can be arranged. The two conformational isomers are I/II,

† This work was supported by the National Science Foundation (Grant MCB-9317369), the Swedish Natural Science Research Council (postdoctoral fellowship to G.C.), and in part by the American Cancer Society (FRA-436).

‡ Present address: Physical Chemistry 2, University of Lund, PO Box 124, S-221 00 Lund, Sweden.

⊗ Abstract published in *Advance ACS Abstracts*, February 15, 1996.

[1] Abbreviations: HJ, Holliday junction; NMR, nuclear magnetic resonance; EDTA, ethylenediaminetetraacetic acid; Tris, tris(hydroxymethyl)aminomethane; 1D, one-dimensional; 2D, two-dimensional; 3D, three-dimensional; NOE, nuclear Overhauser effect; 2Q, two-quantum spectroscopy; TOCSY, total correlation spectroscopy; NOESY, 2D NOE spectroscopy; JR-NOESY, NOESY spectrum acquired with the observe pulse replaced by a jump−return composite sequence; d_i(A;B), intranucleotide connectivity between protons A and B; d_s(A;B), sequential connectivity between protons A and B, where A is in the 5′ direction relative to B; d_c(A;B), cross-strand connectivity between protons A and B; $d_{c,i}$(A;B), cross-strand intra-base-pair connectivity between protons A and B; $d_{c,s}$(A;B), cross-strand sequential connectivity between protons A and B.

0006-2960/96/0435-3534$12.00/0

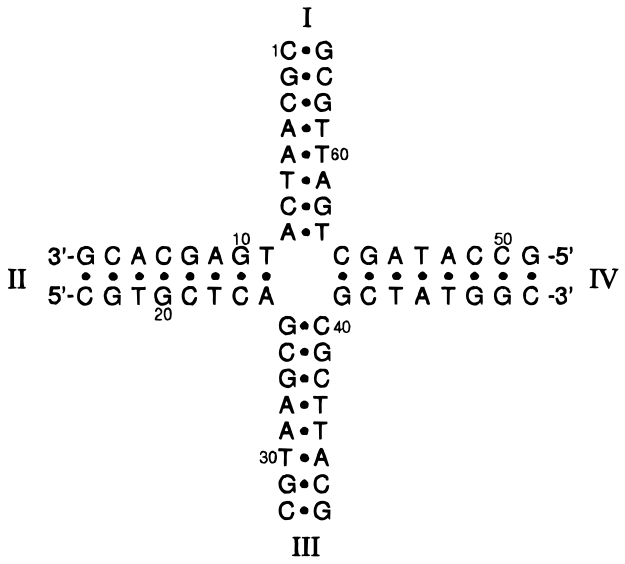

FIGURE 2: The 32-base-pair model Holliday junction, J2P1. J2P1 is related to the previously studied junction J2 by a one-step clockwise cyclic permutation of the four base pairs at the center of the junction. The oligonucleotide sequence runs consecutively from the 5′ end to the 3′ end of the four strands 1 (1−16), 2 (17−32), 3 (33−48), and 4 (49−64). The four duplex arms are numbered with roman numerals (I−IV). The four base pairs at the center comprise the branching point, and the base pair at the open end of each duplex is referred to as the arm terminus.

arm I stacked with arm II and arm III with arm IV, and I/IV, arm I with arm IV and arm II with arm III (Figure 2). These are distinguished by the pair of strands that cross over from one duplex domain to the other: strands 2 and 4 in the I/II isomer; strands 1 and 3 in the I/IV isomer.

Biophysical characterization of Holliday junctions is severely complicated by the phenomenon of branch migration, which is a consequence of the high degree of homology between the two cross-ligated DNA duplexes. To circumvent this problem, Seeman (1982) proposed the study of immobile HJs, composed of DNA strands in which the symmetry of the base sequence is broken. They designed four 16-residue oligomers that upon annealing in the presence of Mg^{2+} were found to form a stable four-arm junction (J1; Seeman & Kallenbach, 1983). Several synthetic immobile junctions have since been designed and studied using an array of biophysical techniques [for reviews see Lilley and Clegg (1993a,b) and Seeman and Kallenbach (1994)].

A consensus view of HJ structure has evolved: in the presence of stabilizing cations (particularly Mg^{2+}), the four duplex arms form two neatly stacked coaxial duplex domains in a scissored X configuration (120°), with two contiguous strands running antiparallel to each other and two strands crossing between stacking domains (Figure 1). Molecular mechanics calculations suggest that this stacked X structure has distorted B-DNA geometry at the junction with widening of the minor groove (von Kitzing *et al.*, 1990). The variability in the scissor angle has been demonstrated by time-resolved laser fluorescence spectroscopy (Eis & Millar, 1993) and examined computationally (Srinivasan & Olson, 1994). Full base pairing for all residues including those at the branching point was suggested on the basis of CD and ^{1}H NMR studies (Wemmer *et al.*, 1985; Marky *et al.*, 1987). In-depth ^{1}H NMR analysis of J1 and a second model HJ related by a simple exchange of two base pairs at the junction (J2) firmly established full base pairing and revealed an apparent sequence dependence to the conformational equilibrium between the two crossover isomers (Chen *et al.*, 1993; Chen & Chazin, 1994). A strong (>10:1) bias toward the I/II isomer was estimated for J1, but was significantly less pronounced (~5:1) for J2. This equilibrium distribution model is consistent with all published results and recent time-resolved fluorescence resonance energy transfer experiments on J1 and J2 (M. Yang and D. P. Millar, in preparation).

In this study, we extend the ^{1}H NMR analysis of synthetic immobile Holliday junctions to examine the hypothesis that the crossover isomer preference is determined solely by the sequence of the four base pairs at the branching point, i.e. independent of the rest of the sequence in the duplex arms, even the adjacent base pair. This has been achieved by constructing a version of the previously studied J2 structure with the four base pairs at the branching point permuted by a single-step clockwise rotation (Figure 2). If the hypothesis is correct, then J2P1 should exhibit a crossover isomer preference opposite to that of J2. A selectively ^{15}N-labeled sample of J2P1 was prepared in the course of this analysis, in an effort to produce a direct monitor of crossover isomer distribution.

MATERIALS AND METHODS

Sample Preparation. Oligonucleotides were synthesized on a 10 μmol scale using an Applied Biosystems 380B DNA synthesizer using solid-phase β-cyanoethyl phosphoramidite chemistry. After deprotection, the oligonucleotides were desalted on a Sephadex G-25 column (NAP™-25, Pharmacia) and purified by FPLC on a Q-Sepharose column (Pharmacia) in 10 mM NaOH with a gradient of 0.4−0.7 M NaCl. The oligonucleotides were then desalted by ultrafiltration (Amicon YC05) rinsing 5−6 times with glass-distilled H_2O, lyophilized, and redissolved in 420 μL Glass-distilled H_2O. The approximate concentration was determined by UV absorption, using the following extinction coefficients at 260 nm (calculated from the molar extinction coefficients for the individual nucleotides): strand 1, 171 600 M^{-1} cm^{-1}; strand 2, 166 300 M^{-1} cm^{-1}; strand 3, 160 100 M^{-1} cm^{-1}; strand 4, 166 900 M^{-1} cm^{-1}. 1D ^{1}H NMR spectroscopy at 348 K was used to check the purity of the stock solutions of the four single strands, monitoring resonances in the base and methyl regions. A 0.45 μmol amount was taken from each of the stock solutions, and pairs of half-complementary strands were titrated together (strand 1 with 4, strand 2 with 3) to within a few percent of a 1:1 molar ratio, as monitored by 1D ^{1}H NMR at 348 K. Next, the 1/4 and 2/3 solutions were titrated to give a mixture of approximately 1:1:1:1 molar ratio of the four oligonucleotides. Formation of the junction was verified by native polyacrylamide gel electrophoresis (PhastGel, Pharmacia) in the presence of 11 mM $MgCl_2$ in both the gel and the buffer media. The single strands, half-complementary duplexes, and three-strand and four-strand structures were all found to have distinct gel mobilities. Buffer strips for gel electrophoresis contained 0.88 M L-alanine, 0.25 M Tris-base, and 11 mM $MgCl_2$. In order to exchange the buffer in the prefabricated gels (Pharmacia Homogenous 20), they were prerun for 150 Vh with the magnesium-containing buffer before the samples were applied.

The solution of the four DNA strands was lyophilized and redissolved in 420 μL of stock buffer [20 mM Tris-d_{11} (MSD

Isotopes) at pH 7.5, 50 mM NaCl, 5 mM $MgCl_2$, 0.2 mM EDTA, 0.003% NaN_3] and 21 μL of D_2O, giving a final concentration of ~l mM J2P1. The sample was annealed by heating at 363 K for 1 min and allowing the solution to cool slowly to room temperature. The experiments in D_2O were acquired after lyophilizing and redissolving three times in D_2O of increasing atomic enrichment (99.9%, 99.96%, and 99.996% D, MSD Isotopes). A second sample of J2P1 with a selectively labeled [1,3-^{15}N]thymine residue in position 9 was prepared as above. The ^{15}N-labeled thymidine phosphoramidite was synthesized by the National Stable Isotope Resource at the Los Alamos National Laboratory (supported by NIH Grant RR02231), and the corresponding DNA strand was prepared by Dr. T. Schmidheini (Microsynth Inc., Windisch, Switzerland).

NMR Spectroscopy. NMR experiments were performed on a Bruker AMX-600 spectrometer. A series of JR-NOESY experiments were acquired in H_2O at five temperatures (285, 293, 296, 300 and 305 K) using the standard pulse sequence (Jeener *et al.*, 1979; Macura & Ernst, 1980; Bodenhausen *et al.*, 1984) with a jump-and-return read pulse (Plateau & Guéron, 1982) to suppress the H_2O resonance and a 200 ms mixing time. The JR excitation sequence was adjusted to position the second excitation maximum in the middle of the imino proton resonances.

After the sample was transferred into D_2O, 2Q ($\tau_e = 30$ ms) (Braunschweiler *et al.*, 1983), TOCSY ($\tau_{sl} = 49$ ms) (Braunschweiler & Ernst, 1983), and NOESY ($\tau_m = 200$ ms) spectra were acquired at 305 K. The residual HOD was suppressed by weak presaturation during the 1.0−1.4 s relaxation delay and during the mixing period of NOESY experiment. The TOCSY experiment was recorded using the modification described by Rance (1987) with a DIPSI-2 sequence (Shaka *et al.*, 1988) for the isotropic mixing. A Hahn-echo was inserted after the read pulse in the TOCSY and NOESY experiments to improve the quality of the base line (Rance & Byrd, 1983; Davis, 1989).

The TOCSY and NOESY experiments were acquired with sine-modulation in t_1 (Otting *et al.*, 1986) and TPPI (Drobny *et al.*, 1979; Bodenhausen *et al.*, 1980) to achieve quadrature detection in the indirectly detected dimension. All 2D experiments were acquired with 96 scans per t_1 value and the following values of t_{1max}: JR-NOESY, 25 ms; 2Q, 25 ms; TOCSY, 44 ms; NOESY, 42 ms. Each NOESY experiment was transformed several times, using different apodization windows to enhance either sensitivity or resolution. The spectra with high resolution were generally processed with a Lorentzian-to-Gaussian window function, whereas enhanced sensitivity was achieved by using a cosine-bell window function.

A 3D homonuclear ^{1}H TOCSY−NOESY experiment (Oschkinat *et al.*, 1988, 1989) was acquired at 305 K with $\tau_{sl} = 48$ ms and $\tau_m = 120$ ms. The mixing periods were set on the basis of cross-peak intensity observed in a series of 2D analogs of the 3D pulse sequence with varying mixing and spin−lock periods. In addition to presaturation during the relaxation delay, weak irradiation of the HOD resonance was performed during the NOESY mixing time. The DIPSI-2 sequence (Shaka *et al.*, 1988) was used for isotropic mixing, in the manner described by Rance (1987). Quadrature detection in the two indirectly detected dimensions was achieved using the method of TPPI-States (Marion *et al.*, 1989). The 3D data set was recorded with 64/126/512 complex points in $t_1/t_2/t_3$, 16 scans per t_1/t_2 value, $t_{1max} = 12$ ms, and $t_{2max} = 24$ ms, for a total experimental time of ~3.5 days. The data set was processed in the order ω_3, ω_1, ω_2. Data points in the t_1 and t_2 dimensions were extended using complex linear prediction, and the first data points in the ω_3 dimension were multiplied by 0.5 to reduce t_1/t_2 noise (Otting *et al.*, 1986). Window functions of sine-bell shifted 75°, sine-bell shifted 70°, and squared cosine-bell were used for the ω_1, ω_2, and ω_3 dimensions, respectively. After zero-filling, the final processed matrix was 256 × 256 × 512 points.

^{15}N−^{1}H correlation experiments were recorded from a 1 mM [1,3-^{15}N]T_9-J2P1 sample on a Bruker AMX 500 spectrometer as 1D ^{15}N-filtered ^{1}H spectra (Griffey *et al.*, 1983). These experiments were recorded with a refocusing delay inserted after the last ^{15}N pulse to allow ^{15}N GARP decoupling (Shaka *et al.*, 1985) during acquisition. Spectra were acquired at 276, 280, 285, 290, 295, and 300 K.

The data were processed on a SUN SPARCstation IPX or a SPARCstation 2 using version 2.05 or 2.1 of FELIX (Biosym, Inc.). All chemical shifts are reported at 305 K (unless otherwise stated) and are referenced to the H_2O resonance at 4.68 ppm (Hartel *et al.*, 1982; Orbons *et al.*, 1987).

RESULTS AND DISCUSSION

Evidence for the formation of the J2P1 junction was obtained from polyacrylamide gel electrophoresis run in the presence of Mg^{2+} ions. The gel also showed the presence of a small amount of half-complementary duplexes in the sample of J2P1, giving rise to a number of weak and sharp spurious peaks, especially in the 2Q and TOCSY spectra. These extra peaks caused only minor complications in the assignment procedure, as they were of much lower intensity in the NOESY spectra.

Using the ^{1}H resonance assignment strategy outlined below, we have been able to obtain virtually complete sequential assignments of the nonlabile 2H, 5H, $5CH_3$, 6H, and 8H base resonances, the 1′H, 2′H, 2′′H, and 3′H sugar resonances, and the labile cytosine $4NH_2$, guanine N1H, and thymine N3H base resonances. The few missing assignments were all from residues at or near the junction, whose resonances tended to be broad and very weak. We use the shorthand notation described by Wüthrich (1986) to specify distances and the corresponding NOE connectivities. Intraresidue and sequential (5′ to 3′ direction) NOEs are indicated by d_i(A;B) and d_s(A;B), respectively. Cross-strand NOEs are indicated by d_c(A;B).

Assignment Strategy. ^{1}H NMR sequential resonance assignments for a 64-residue, ~20 000 Da HJ are severely complicated by the large size of the molecule, which causes broad resonance lines and substantial overlap in certain spectral regions. Thorough descriptions of the assignment procedures used for HJs J1 and J2 have been published (Chen *et al.*, 1991, 1993; Chen & Chazin, 1994). In short, 2Q and TOCSY experiments are used for identification of the sugar ring, cytosine 5H/6H and thymine $5CH_3$/6H scalar-coupled spin systems, and data from NOESY experiments are used for the subsequent pairing of bases and sugars and for the sequential ordering of the residues. All potentially useful areas of the NOESY spectra are analyzed in parallel, circumventing problems in one region by finding resolved

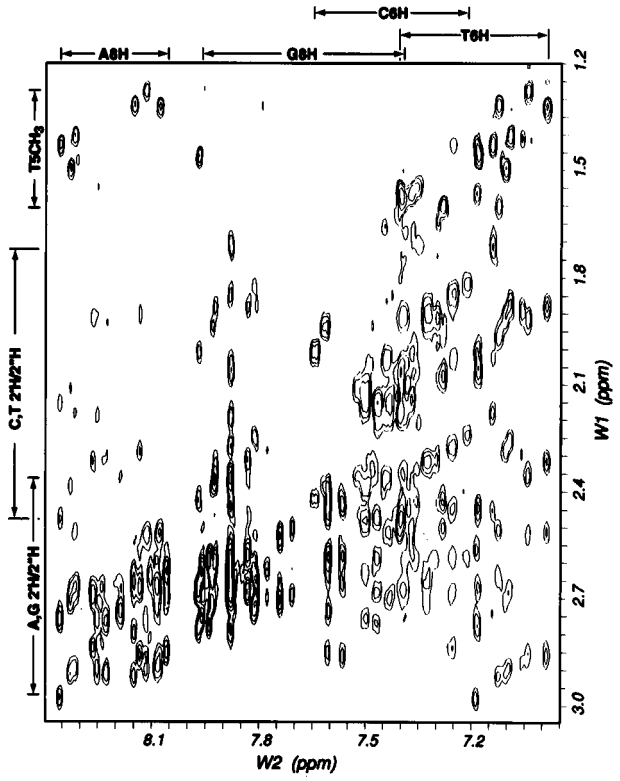

FIGURE 3: Quality of the NMR spectra of the 64-residue structure J2P1. Region of the 600 MHz JR-NOESY(τ_m = 200 ms) spectrum at 305 K of 1 mM J2P1 containing cross-peaks to 6H/8H base protons from 2′H, 2″H, and thymine $5CH_3$. The experimental conditions and acquisition parameters are described in detail in Materials and Methods.

connectivities in another. It is advantageous to allow for some degree of spin diffusion in the NOESY experiments to enable observation of a number of NOE connectivities that are not usually analyzed to make assignments but which offer increased cross-peak resolution for certain nucleotide combinations. Acquisition of spectra over a range of experimental conditions is also critically important. In this study, we have added the 3D TOCSY−NOESY experiment as an efficient means for making sequence assignments, providing both scalar coupling and NOE connectivities in the same experiment as well as much-needed additional cross-peak resolution. In the following section, a short description of the unique aspects of the assignment of J2P1 will be given. A more detailed account is provided as supporting information.

Nonlabile Proton Assignments. The ^{1}H resonance assignments for J2P1 were made using data from the 2Q, TOCSY, NOESY and 3D TOCSY−NOESY experiments acquired at 305 K and were supplemented by a few additional JR-NOESY spectra recorded at lower temperatures. A vast majority of resonances were identified and sequentially assigned using the JR-NOESY and the 3D TOCSY−NOESY experiments. The 2Q and TOCSY experiments were subsequently used to corroborate the tentative assignments obtained from the NOESY and 3D TOCSY−NOESY, and to identify additional 1′H, 2′H, and 2″H resonances. The high sensitivity obtained in the JR-NOESY experiments allowed for data processing with strong resolution enhancement, which proved extremely valuable for disentangling regions with severely overlapped cross-peaks. Figure 3 provides an illustration of the quality of the JR-NOESY spectrum acquired at 305 K, showing the region containing the $d_{i,s}$(2′H,2″H;6H,8H), d_i(6H;$5CH_3$), and d_s(6H,8H;$5CH_3$) NOEs. Careful analyses of this region in parallel with the $d_{i,s}$(1′H,3′H;6H,8H), d_i(6H;5H) and d_s(6H,8H;5H) connectivities allowed for identification of most 6H and 8H base proton resonances as well as a substantial number of the 1′H, 2′H, 2″H, and 3′H resonances. As in our previous studies, a variety of alternative sequential pathways added important complementary information, including: $d_{i,s}$(1′H,2′H,2″H;5H, $5CH_3$), d_s(5H,$5CH_3$;5H,$5CH_3$), and d_s(6H,8H;6H,8H). The ^{1}H resonance assignments for J2P1 are listed in Table 1.

The 3D TOCSY−NOESY experiment was particularly useful for analysis of crowded spectral regions, taking advantage of the increased resolution of cross-peaks obtained by correlating the NOE connectivities to a third spin via scalar coupling (Mooren *et al.*, 1991; Piotto & Gorenstein, 1991; Radhakrishnan *et al.*, 1991). For instance, analyses of the region of the NOESY spectrum containing the intraresidue and sequential cytidine 1′H,2′H,2″H,3′H/6H connectivities, which normally is severely overlapped, is vastly simplified in the 3D spectrum by the additional correlation to the 5H resonance. Figure 4 illustrates the substantial reduction of complexity obtained in the 3D experiment for the NOE connectivities to three overlapped cytosine 5H resonances. The 3D spectrum was also beneficial for confirming many of the assignments obtained from the 2D NOESY spectra.

Two problems were particularly difficult to overcome. First, a number of guanosine residues had identical 8H chemical shifts, which created ambiguity in the identification and attribution of individual cross-peaks. In contrast, the adenine 8H resonances are reasonably well dispersed and could be assigned in a fairly straightforward manner. The second severe assignment problem was for residues A_8, T_9, C_{40}, and G_{41}, all of which are in the critical region of the branching point. For these residues, resonance lines were exchange broadened, and correspondingly, only weak cross-peaks in 2D spectra were observed. For example, no sequential NOEs were found for the severely exchange broadened 6H resonance of C_{40}; its assignment could only be made indirectly on the basis of a broad, low-intensity intraresidue cross-peak to the 5H resonance in NOESY and TOCSY spectra, for which some sequential d_s(1′H,2′H,2″H;5H) NOEs were observed from G_{39}. Similarly, the 6H resonance of T_9 was exchange broadened and could be assigned only indirectly via a weak and broad intraresidue NOESY cross-peak to the sequentially assigned $5CH_3$ resonance. The 8H resonance of G_{41} could only be identified via the 2′H and 2″H resonances of G_{41}, with d_s(2′H,2″H;5H) and d_s(2′H,2″H;6H) NOEs for G_{41}/C_{42} providing markers to identify a weak d_i(2″H;8H) NOE for G_{41}. Assignment of C_7 was also problematical because only one weak sequential connectivity to the exchange-broadened A_8 8H was observed, and the sugar ring protons were not clearly resolved.

A summary of the sequential NOE data for J2P1 obtained from the various NOESY experiments is given in Figure 5, divided into separate categories for 6H/8H and 5H/$5CH_3$ connectivities. Of the 60 possible connectivities between residues (15 per DNA strand for a 32-base-pair Holliday junction), at least one, and for almost all residues many more (Figures S1 and S2 of the supporting information), sequential NOE was identified for all residue pairs except T_9-G_{10} and

Table 1: ^{1}H NMR Resonance Assignments for J2P1 at pH 7.5, 305 K[a]

residue	6H/8H	5H/5CH$_3$/2H	1′H	2′H	2″H	3′H	4′H	4NH(1)	4NH(2)	N1H/N3H
strand 1										
C1	7.61	5.90	5.77	1.93	2.38	4.68	4.07	*	*	
G2	7.92		5.86	2.64	2.72	4.96	*			12.99
C3	7.32	5.42	5.51	1.92	2.30	4.80	*	6.30	8.33	
A4	8.22	7.22	5.94	2.76	2.90	5.04	*			
A5	8.11	7.62	6.13	2.52	2.85	4.96	*			
T6	7.04	1.28	5.80	1.90	2.35	4.78	*			13.37
C7	7.39	5.54	5.56	2.18	*	4.82	*	6.48	8.26	
A8	8.24	7.60	6.23	2.76	2.89	4.99	*			
T9	7.34	1.54	*	*	2.20	4.79	*			13.78[b]
G10	7.88		5.35	2.58	2.70	4.93	*			12.45
A11	8.06	7.62	6.00	2.62	2.84	5.01	*			
G12	7.60		5.68	2.45	2.58	4.92	*			12.76
C13	7.30	5.29	5.57	1.90	2.31	4.80	*	6.22	8.16	
A14	8.26	7.82	6.17	2.68	2.84	5.00	*			
C15	7.25	5.37	5.67	1.84	2.27	4.77	4.13	6.63	8.28	
G16	7.88		6.12	2.35	2.54	4.66	*			*
strand 2										
C17	7.64	5.90	5.79	2.00	2.42	4.70	4.07	*	*	
G18	7.96		5.97	2.66	2.78	4.97	*			12.80
T19	7.18	1.45	5.82	2.05	2.44	4.88	*			13.60
G20	7.88		5.88	2.65	2.68	4.98	*			12.72
C21	7.38	5.33	5.88	2.04	2.48	4.68	*	6.45	8.05	
T22	7.40	1.58	6.00	2.10	2.46	4.84	*			13.74
C23	7.52	5.70	5.49	2.10	2.35	4.83	*	6.83	8.40	
A24	8.18	7.38	6.02	2.65	2.73	4.99	*			
G25	7.60		5.75	2.38	2.58	4.88	*			*
C26	7.21	5.28	5.52	1.81	2.24	4.77	*	6.26	8.20	
G27	7.82		5.42	2.60	2.72	4.96	*			12.63
A28	8.08	7.24	5.96	2.66	2.90	5.04	*			
A29	8.07	7.65	6.11	2.51	2.86	4.98	*			
T30	6.98	1.32	5.72	1.88	2.31	4.82	*			13.46
G31	7.83		5.90	2.57	2.68	4.95	*			12.73
C32	7.46	5.46	6.20	2.14	2.20	4.48	4.06	*	*	
strand 3										
G33	7.94		5.96	2.58	2.76	4.84	*			*
C34	7.46	5.46	5.66	2.14	2.46	4.88	*	6.47	8.36	
A35	8.35	7.70	6.32	2.75	2.97	5.04	4.45			
T36	7.18	1.42	5.92	2.00	2.56	4.81	*			13.62
T37	7.36	1.56	6.04	2.14	2.50	4.87	*			13.71
C38	7.44	5.61	5.62	2.02	2.36	4.85	*	6.72	8.35	
G39	7.88		5.86	2.61	2.71	*	*			12.80
C40	7.48	5.36	*	*	2.34	*	*	6.40	8.16	
G41	7.39		5.70	2.42	2.58	*	*			12.86
C42	7.35	5.16	5.83	2.06	2.45	4.68	*	6.48	8.09	
T43	7.40	1.54	5.68	2.18	2.50	4.86	*			13.44
A44	8.31	7.40	6.24	2.66	2.89	5.01	*			
T45	7.09	1.40	5.64	1.86	2.25	4.82	*			13.47
G46	7.80		5.60	2.64	2.72	4.96	*			12.84
G47	7.74		5.96	2.52	2.70	4.93	*			13.06
C48	7.42	5.44	6.17	2.13	2.20	4.48	4.05	*	*	
strand 4										
G49	7.96		5.98	2.62	2.76	4.82	*			*
C50	7.49	5.40	6.06	2.15	2.48	4.85	*	6.39	8.30	
C51	7.50	5.64	5.43	2.10	2.38	4.85	4.12	6.71	8.45	
A52	8.32	7.66	6.24	2.70	2.91	5.02	4.43			
T53	7.10	1.48	5.52	1.90	2.28	4.82	4.12			13.23
A54	8.13	7.22	6.01	2.66	2.86	5.00	*			
G55	7.56		5.74	2.43	2.58	4.88	*			12.83
C56	7.25	5.07	5.87	2.02	2.44	4.74	*	6.28	8.06	
T57	7.14	1.42	5.66	1.70	2.18	4.79	*			*
G58	7.88		5.55	2.68	2.80	*	*			*
A59	8.14	7.68	6.22	2.63	2.92	4.98	*			
T60	7.12	1.31	5.88	1.95	2.50	4.81	*			13.60
T61	7.28	1.60	5.82	2.06	2.42	4.88	*			13.70
G62	7.88		5.82	2.60	2.67	*	*			12.63
C63	7.32	5.41	5.78	1.88	2.30	4.79	4.15	6.50	8.39	
G64	7.92		6.14	2.36	2.58	4.67	*			*

[a] Chemical shifts referenced to the residual HOD signal, precalibrated using methanol (Hartel *et al.*, 1982; Orbons *et al.*, 1987). The symbol "*" indicates no assignment for the resonance. [b] Chemical shift value obtained from 1D ^{15}N-filtered experiment of ^{15}N-labeled sample.

C_{40}-G_{41} (open boxes on line b in Figure 5). All of these residues except G_{10} are directly at the branching point and exhibit broad, low-intensity cross-peaks. Assignment of sequential NOEs to the 8H resonance of both G_{10} and G_{41}

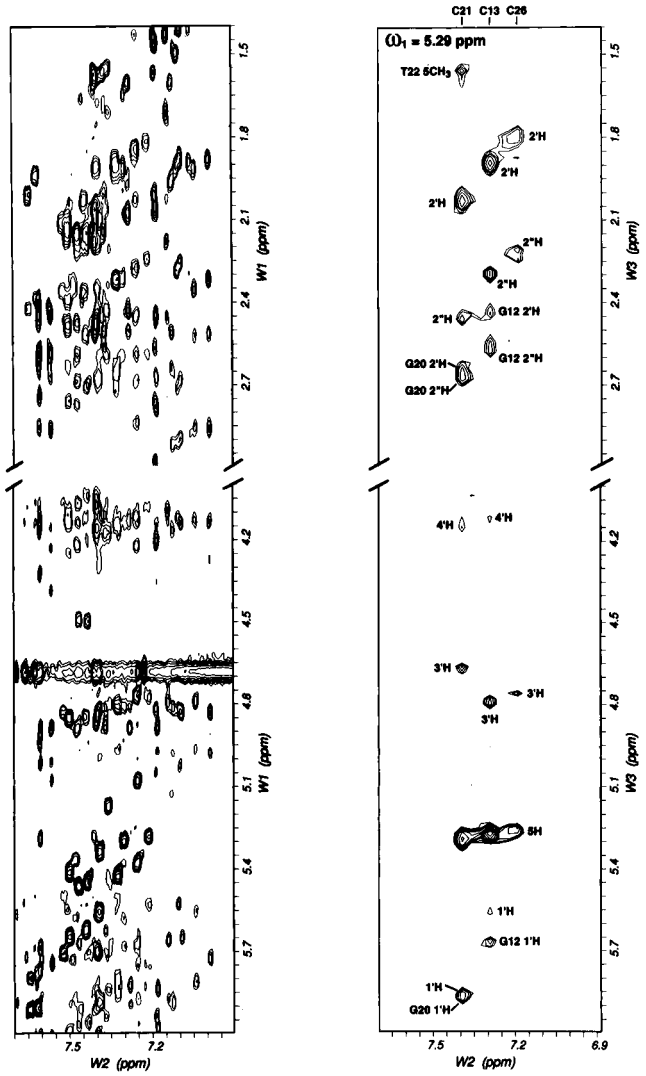

FIGURE 4: Spectral simplification from 3D NMR. Corresponding regions from (a) the 2D JR-NOESY(τ_m = 200 ms) spectrum at 305 K of 1 mM J2P1 in H_2O and (b) the ($\omega 2$,$\omega 3$) plane at ω_1 = 5.29 ppm of a 3D TOCSY−NOESY (τ_{sl} = 48 ms/τ_m = 120 ms) spectrum at 305 K of the same sample in D_2O. These plots contain cross-peaks between 6H/8H base protons and sugar ring protons and cytosine 5H base protons. In the 3D spectrum, the three cytosine 6H proton frequencies are indicated at the top. Inter-residue cross-peaks are identified by residue and proton assignment, intraresidue peaks by proton assignment only.

was further complicated by severe spectral crowding: five other guanine 8H resonances are degenerate with G_{10}; although G_{41} 8H is shifted far upfield relative to all other guanosine residues, it resonates within 0.03 ppm of six cytosine and thymine 6H signals.

Labile Proton Assignments. The strategy for sequential assignment of the labile protons of J2P1 was as described in Chen *et al.* (1993). The very low field shifted imino proton resonances of thymine and guanine are differentiated on the basis of chemical shift (T > 13.25 ppm > G) and characteristic intra-base-pair NOEs to adenine 2H and cytosine $4NH_2$ resonances, respectively. The most direct information about the sequential order of the base pairs comes from observation of connectivities between adjacent imino protons. Direct sequential NOEs also arise from the short inter-base-pair distances d_s(2H;N1H,N3H) and d_s(N1H, N3H;$4NH_2$). More indirect pathways for assignment are also available following connectivities involving the adenine 2H

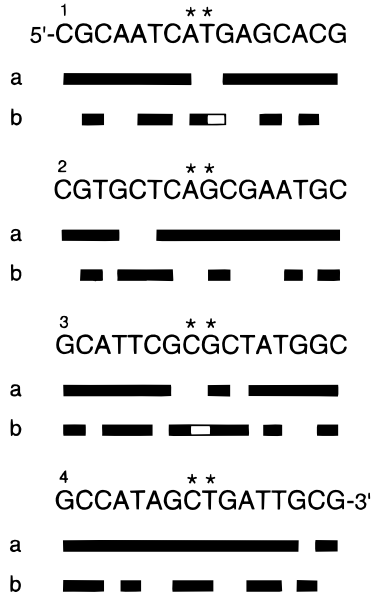

FIGURE 5: Summary of sequential NOE cross-peaks involving the nonlabile protons of J2P1 observed in 2D NOESY and 3D TOCSY−NOESY spectra obtained at 285, 293, 296, 300, and 305 K. A line between residues is drawn in row "a" when at least one of the d_s(1′H,2′H,2″H;6H,8H) NOEs was assigned. The d_s(1′H,2′H,2″H,6H,8H;5H,5CH_3) NOEs are indicated in row "b". An open bar indicates that no NOE was identified. "∗" indicates residues at the branching point.

[e.g., inter-base-pair d_s(2H;2H), intraresidue d_i(1′H;2H), inter-base-pair d_c(1′H;2H), sequential d_s(1′H;2H), and cross-strand sequential $d_{c,s}$(1′H;2H)], cytosine 5H and thymine 5CH_3 [e.g., intra-base-pair $d_{c,i}$(N1H;5H), d_i(N3H;5CH_3), and inter-base-pair d_s(N1H,N3H;5H,5CH_3)]. The cytosine $4NH_2$ protons are readily characterized by their chemical shifts, strong NOE between them, and intraresidue NOEs to 5H (and 6H via spin diffusion). At least one sequential connectivity was identified for all base pairs except the four-arm termini and two base pairs directly at the junction (C_{40}/G_{25} and C_{56}/G_{41}; Figure S3). In the studies of J1 and J2 (Chen *et al.*, 1993), the chemical shift for the imino protons of the residues at the branching point could be identified, showing that these residues were base paired. We were unable to identify the imino protons of residues directly at the junction in J2P1 using these same methods, presumably due to exchange-broadening effects. However, the imino proton of T_9 was identified in the ^{15}N-filtered ^{1}H experiments on the ^{15}N-labeled sample of J2P1 (*vide infra*), showing that at least this residue is base paired. All observed imino and amino proton resonate in regions characteristic for Watson−Crick type base pairing. Given the extensive similarities among J1, J2, and J2P1, we feel safe in assuming that all of the residues in J2P1 are base paired.

Conformation within the Duplex Domains. Careful comparison of the intensities for the d_i(2′H,2″H;6H,8H) and d_s(2′H,2″H;6H,8H) connectivities in the NOESY (200 ms) and 3D TOCSY−NOESY (120 ms) spectra revealed that several residues show differences from what is expected from standard B-DNA conformation. For residues in the junction this was not surprising as the conformation of these residues might very well be distorted, but for residues away from the junction, this is not expected. For standard B-type DNA, the relative intensities are d_i(2′H;6H,8H) > d_s(2″H;6H,8H) > d_i(2″H;6H,8H) > d_s(2′H;6H,8H), whereas for J2P1, d_i(2′H;6H,8H) > d_i(2″H;6H,8H) > d_s(2″H;6H,8H) >

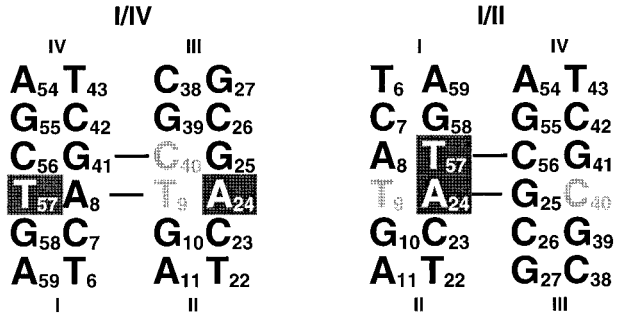

FIGURE 6: Organization of residues at and near the branching point for the I/II and I/IV crossover isomers of J2P1, illustrating the difference in spatial proximities of A_{24}/T_{57} and T_9/C_{40}. The crossover linkage is indicated by the horizontal lines.

d_s(2′H;6H,8H) is observed for many residues. This trend is not compatible with any right-hand DNA helix. We initially ascribed these observations to spin diffusion arising during the rather long mixing times used in the two NOESY experiments. However, NOESY experiments acquired with shorter mixing times appear to have the same relative intensities (S. Miick and W. J. Chazin, unpublished results). One possible explanation for the anomalous *d*(2′H,2″H;6H, 8H) intensities is that dipolar vectors corresponding to the intraresidue and sequential NOEs have different effective motions (correlation times). This can arise from either anisotropic overall tumbling or an anisotropic second motion with a correlation time of the order of the overall tumbling of the molecule. Investigations into the origins of this effect are currently underway in this laboratory. As a result of these complications we have resorted to an alternative approach to check for the existing DNA conformation, comparing the relative intensities of d_s(1′H;6H,8H) and d_s(3′H;6H,8H) NOEs. For A-form DNA d_s(3′H;6H,8H) = 3.0−3.1 Å < d_s(1′H;6H,8H) = 4.6 Å, whereas for B-form DNA d_s(3′H;6H,8H) = 4.6 Å > d_s(1′H;6H,8H) = 3.5−3.6 Å (Wüthrich, 1986). Careful comparison of these NOE intensities for J2P1 shows that in all cases the d_s(1′H;6H, 8H) NOE has greater intensity than the d_s(3′H;6H,8H), indicative of B-type geometry.

Stacking Geometry of the Duplex Arms. The arm-stacking geometry can be determined from characteristic sequential NOEs involving the eight residues at the branching point (Macke *et al.*, 1992). The two types of strands in a branched DNA structure, contiguous and crossover, are expected to give rise to different patterns of sequential NOE connectivities at the branching point. Standard B-form sequential NOEs are expected along the contiguous strand. For the crossover strand, the standard sequential-type NOE connectivities are expected, but these would be between residues that are not adjacent in sequence. Thus, connectivities between residues on the two crossover strands are particularly informative as they directly implicate a specific arm-stacking arrangement (Figure 6).

Table 2 lists all unambiguously identified cross-peaks involving the eight branching point residues. Two general observations were made from the analysis of the sequential NOEs along each strand in the region of the branching point. First, the sequential NOEs between A_8 and T_9 in strand 1 are of considerably lower intensity than the corresponding NOEs between A_{24} and G_{25} in strand 2 or between C_{56} and T_{57} in strand 4. (The analysis for C_{40} and G_{41} in strand 3 is not clear-cut because the chemical shift for G_{41} 8H is in a severely crowded region of the spectrum and the 1′H and 2′H protons of C_{40} could not be unambiguously identified.) Second, the usual complement of sequential connectivities were observed for the residues at the branching point in strands 2 and 4 but not in strands 1 and 3 (Figure 5). Thus, strands 2 and 4 adopt a more regular B-DNA conformation across the branching point and must be contiguous strands, and strands 1 and 3 cross over from one stacking domain to the other. In addition to these intrastrand NOEs, a number of NOEs between residues that are not adjacent in the sequence are observed, including several between T_9 and C_{40}. These connectivities are only consistent with arm I stacking with arm IV and with arm II stacking with arm III. Together, the NOE data indicate a predominance of the I/IV crossover isomer. Corresponding observations have been made for J1 and J2 (Chen & Chazin, 1994), although the data indicate a preference for the I/II crossover isomer.

Table 2: Unambiguously Assigned NOE Cross-Peaks between Junction Residues of J2P1

I/IV (major)	I/II (minor)
A_{24}/G_{25}	A_8/T_9
1′H/8H	2′H/5CH_3
2′H/8H	2″H/5CH_3
2″H/8H	3′H/5CH_3
3′H/8H	
8H/8H	
C_{56}/T_{57}	A_{24}/T_{57}
1′H/5CH_3	2′H/5CH_3
2′H/5CH_3	2″H/6H
2″H/5CH_3	3′H/6H
3′H/5CH_3	
5H/5CH_3	
6H/5CH_3	
1′H/6H	
3′H/6H	
T_9/C_{40}	
5CH_3/1′H	
5CH_3/2′H	
5CH_3/5H	
5CH_3/6H	

To complete the analysis of the NOE data for J2P1, it is necessary to rationalize the presence of uniformly weak but unambiguous NOE connectivities that are inconsistent with the predominant I/IV arm-stacking geometry. A schematic diagram of the two crossover isomers is provided in Figure 6 to facilitate the discussion. The set of weak NOEs corresponds to sequential connectivities at the branching point of strand 1 and interstrand connectivities between A_{24} and T_{57}. The latter are particularly informative, as even with substantial distortion in the I/IV isomer it is not possible to bring A_{24} and T_{57} in close enough proximity to give rise to a NOE between them. Conversely, the minor set of connectivities is fully compatible with a I/II stacking geometry. Since only one set of resonance frequencies is observed for J2P1, these results imply that the two crossover isomers coexist in solution in fast exchange on the NMR chemical shift time scale, with the I/IV isomer predominating.

Although the chemical shift parameter is difficult to interpret directly, structural insights can be obtained from a qualitative analysis. The bulk of the chemical shifts of J2P1 is fully consistent with normally stacked standard B-type conformation. However, the chemical shifts of a few base protons in arm IV in the region of the branching point are significantly perturbed. For example, the resonances of C_{42} 5H and G_{41} 8H in the crossover strand, as well as the 5H

resonance of C_{56} in the contiguous strand, are uniquely high-field shifted at 5.16, 7.39, and 5.07 ppm, respectively. The chemical shifts in DNA are quite sensitive to base-stacking interactions, a consequence of the strong ring current effect from nearby aromatic rings. The unusual chemical shift values observed for these residues are indicative of *perturbed base-stacking interactions at and adjacent to the branching point for arm IV*.

The issue of base-stacking interactions at the HJ branching point has been raised as a critical point in understanding the results of experiments probing HJ structure (Cooper & Hagerman, 1991). The cumulative results from our analyses of the chemical shift and NOE data on J1, J2, and J2P1 indicate that the bases in the region of the branching point in the contiguous strands are stacked in a B-form-like manner. In the crossover strands, while there is less data due to the exchange-broadening effects on resonance lines, the NOE and chemical shift evidence clearly point to some form of distortion in the stacking of bases in the region of the branching point. The presence of perturbed base stacking is in disagreement with the computational analysis by Srinivasan and Olson (1994), who found structural deformation only in the DNA backbone.

Direct Assay of the Isomer Distribution by Heteronuclear NMR. Broadening of ^{1}H resonance lines is evident for residues at the branching point of J2P1, a phenomenon that has been observed for all of our model HJs studied so far (Chen *et al.*, 1991, 1993; Chen & Chazin, 1994). Large effects are observed for certain resonances of the crossover strands, but little if any are observed on resonances in the contiguous strands. For J1 and J2, the phenomenon is temperature dependent with resonances sharpening somewhat as the temperature is lowered from 310 K, and a similar trend is observed for J2P1. This line-broadening effect has been attributed to local fraying of the base pairs and/or to conformational heterogeneity of the junction.

To gain further information on the origin of the line-broadening effects, a series of 1D ^{15}N-filtered ^{1}H-detected experiments on the sample of [1,3-^{15}N]T_9-J2P1 were acquired at different temperatures (Figure 7). In addition to identifying the chemical shift of the imino proton of residue T_9, the spectra clearly reveal the appearance of a second ^{1}H resonance in the base-paired region at temperatures below 300 K. This indicates that at lower temperatures, line broadening arises from conformational heterogeneity and confirms the hypothesis derived from the NOE analysis, that J2P1 exists in solution as an equilibrium distribution between the two crossover isomers. The ratio of the signal intensity of the major and minor signal is approximately 5:1 at 280 K, consistent with the rough estimate based on NOE intensities. The apparent line narrowing observed as the temperature is lowered from 310 to 300 K is probably due to a reduction in local base-pair fraying at the strained branching point.

Crossover Isomer Preference Is Governed by Sequence at the Branching Point. An analysis of the ^{1}H chemical shifts observed for J2 and J2P1 provides further insight into the structures of the HJs at the local level and the dependence on sequence at the branching point. A graphical comparison of the chemical shift data for two of the HJs we have studied (J2, J2P1) is presented in Figure 8. The great similarity of the ^{1}H chemical shifts for all residues except those at the branching point suggests that the local conformation in the

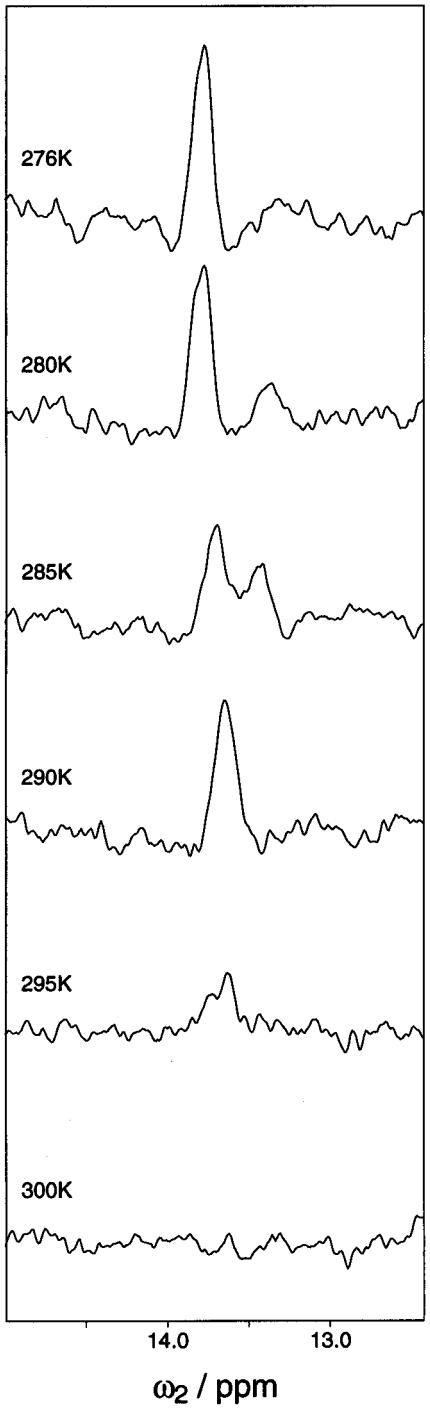

FIGURE 7: The model HJ J2P1 exists as an equilibrium mixture of two conformers. Temperature dependence of the 1D ^{15}N-filtered spectra of 1 mM J2P1. The sample was prepared with a single [1,3-^{15}N]thymidine label at T_9, directly at the site of junction crossover point. The experimental conditions and acquisition parameters are described in detail in Materials and Methods.

duplex arms of these two HJs are very similar. The comparative analysis of NOEs observed for J2 and J2P1 shows that the single-step cyclic permutation of J2 with respect to its four duplex arms does cause the anticipated change in the crossover isomer preference from I/II to I/IV. Thus, it appears that the crossover preference is determined by the sequence at the branching point, and that the penultimate residue is playing, at best, only a minor role. Further experiments are underway to evaluate if the n-1 residue has any effect on the crossover isomer distribution.

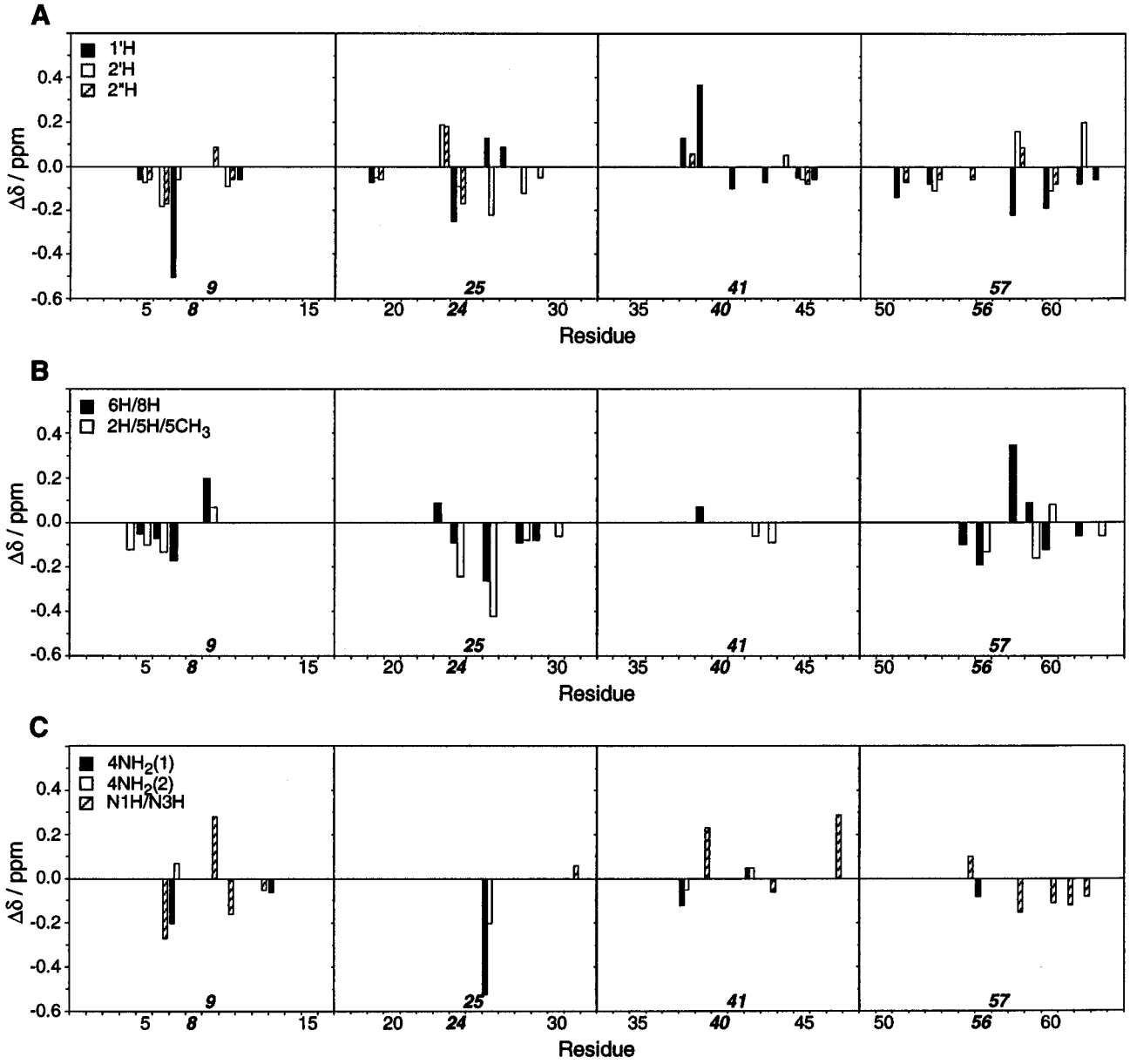

FIGURE 8: Chemical shift comparison between Holliday junctions J2P1 and J2. The significant chemical shift differences are plotted as δ(J2P1) − δ(J2) for (A) 1′H (solid bars), 2′H (open bars), and 2″H (hatched bars); (B) 6H/8H (solid bars) and 2H/5CH3/5H (open bars); (C) 4NH(1) (solid bars), 4NH(2) (open bars), and N1H/N3H (hatched bars). The chemical shifts for J2 are those reported at 310 K (Chen *et al.*, 1993; Chen & Chazin, 1994).

Comparison of Four-Stranded HJs and a Single-Strand Cruciform. A new and interesting alternative approach for the construction of a four-way junction has recently been presented (Pikkemaat *et al.*, 1994). Instead of using four separate oligomers, these authors incorporated three highly stable H2-type mini-hairpin loops into a single DNA strand with a base sequence specifically designed to facilitate formation of a four-arm cruciform structure. ^{1}H NMR showed that a branched structure was formed in the presence of Mg^{2+}. The high stability of the hairpin loops allows shorter individual duplex arms to be used, thereby reducing the size of the molecular aggregate and facilitating NMR studies.

In this 16-base-pair cruciform junction (HJC16), the disposition of residues at the branching point is closely related to J2 and J2P1, and, as anticipated, the preferred crossover isomer is consistent with the results obtained for J2 and J2P1 (Figure 9). However, comparison of the ^{1}H chemical shifts of corresponding protons reveals some very large differences among the residues at the branching point (Table 3). Two residues are situated in identical positions in all three junctions, namely, $T_{57}/T_9/T_{18}$ and $A_8/A_{24}/A_9$ in J2P1/J2/HJC16, respectively, and comparison of their chemical shifts shows that the values in HJC16 differ from those found for the other two HJs. Further comparisons of HJC16 chemical shifts to those for identical residues in homologous positions in J2P1 (C_{19}/C_{56}, G_{28}/G_{41}) and J2 (T_8/T_{25}, A_{39}/A_{40}, C_7/C_{26}, G_{40}/G_{39}) also show significant differences. Of particular note are very unusual downfield shifts for the base proton resonances of residues at the branching point in the two crossover strands of HJC16. For instance, the C_{29} 5H chemical shift of 5.84 ppm is a value normally observed for cytosine residues at the 5′ arm terminus, and the T_8 $5CH_3$ chemical shift of 1.69 ppm occurs in the region common to methyl protons of thymine residues in a single-stranded stack or nonstructured conformation (Altona, 1990). The 6H resonances for these two residues are also extremely downfield shifted in HJC16, as are G_{28} 8H and C_{19} 5H. Since

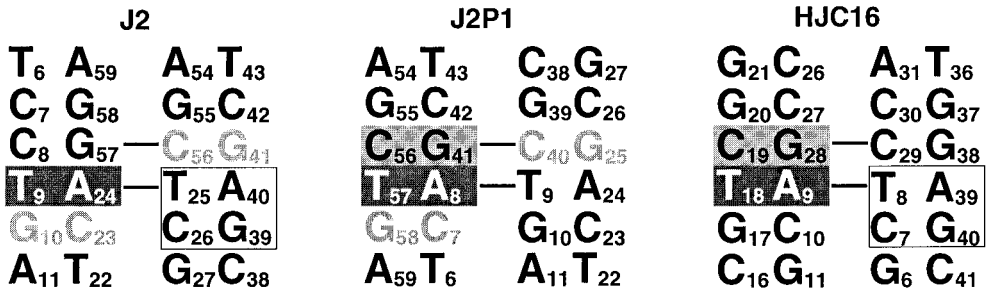

FIGURE 9: Schematic overview of the branching point of J2, J2P1, and HJC16 for the predominant stacking conformations. Residues in identical sequence contexts are highlighted: the TA base pair common to all three junctions has a dark gray background; the two CG base pairs common to J2 and J2P1 are printed in light gray; the TA and CG base pairs common to J2 and HJC16 are enclosed in a box; the CG base pair common to J2P1 and HJC16 has a light gray background. The crossover linkage is indicated by the horizontal lines.

Table 3: Chemical Shift Comparisons for Residues of J2P1, J2, and HJC16 that Occupy Homologous Positions at and Adjacent to the Branching Point[a]

	6H/8H	2H/5H/5CH$_3$	1′H	2′H	2″H	3′H
J2P1-J2						
C_7/C_{23}	−	−0.14	−	0.27	*	−
A_8/A_{24}[b]	−	−	−	−	−	*
G_{25}/G_{41}	*		−	*	*	*
C_{40}/C_{56}	−	0.16	*	*	−	*
T_{57}/T_9	−	−	−	−	−	−
G_{58}/G_{10}	−		−0.22	−	−	*
J2P1-HJC16						
A_8/A_9	0.42	−	0.14	0.14	0.11	−
G_{41}/G_{28}	−0.71		−0.46	−0.14	−0.62	*
C_{56}/C_{19}	−0.12	−0.45	−	0.27	0.19	−0.11
T_{57}/T_{18}	−0.16	−	−0.36	−0.47	−0.41	−
J2-HJC16						
T_9/T_{18}	−0.16	−	−0.34	−0.54	−0.48	−
A_{24}/A_9	0.45	−	0.18	0.12	0.12	*
T_{25}/T_8	−0.31	−0.20	−0.30	−0.38	−0.47	*
C_{26}/C_7	−	0.36	−0.59	−	−0.17	−0.10
G_{39}/G_{40}	0.11		0.19	0.11	0.13	−0.12
A_{40}/A_{39}	0.19	*	−	0.23	−	*

[a] The "*" symbol indicates that the assignment was not available for at least one of the two HJs. The "−" symbol indicates that the chemical shift difference is less than 0.1 ppm. [b] Bold-type residues indicate identical positions in all three junctions. The chemical shift values for J2 were measured at 310 K, pH 7.5 (Chen & Chazin, 1994), and at 302 K, pH 7.0 (Pikkemaat *et al.*, 1994), for HJC16.

the chemical shifts of the base protons are dominated by ring currents arising from base stacking, the local structure at the branch point of the 16-base-pair cruciform must be different from that of J2 and J2P1. Given the trend toward single-strand or nonstructured conformation, it appears that HJC16 does not have optimal base-stacking interactions at the branch point. This effect may arise from the presence of the highly structured stable hairpin loops being clamped on to very short duplex arms, which may induce additional strain into the molecule via perturbation of the local conformation at the branching point. By analogy, this finding may have important implications on some of the elegant work by Seeman and co-workers using constrained HJ systems [e.g., Fu and Seeman (1993), and Zhang and Seeman (1994)]. The potential for problems associated with conformational strain in these systems has been recognized (Zhang & Seeman, 1994).

CONCLUDING REMARKS

In this study, we have extended the ^{1}H NMR analysis of synthetic immobile Holliday junctions to a variant of J2 which corresponds to a simple clockwise cyclic permutation of the four base pairs at the branching point. It is found that the change in the order of the base pairs does indeed cause a change in the preferred stacking arrangement of J2P1 relative to J2. Observation of several interbase NOEs clearly indicate a preference for the I/IV crossover isomer, but, just as for J2, observation of a few additional weak NOE connectivities indicates the presence of a small quantity of the alternative (I/II) isomer as well. Further results from 1D ^{15}N-filtered ^{1}H-detected experiments at low temperatures on a specifically labeled sample of J2P1 gives direct support for the co-existence of the two crossover isomers and provides a much more direct and accurate measure of the isomer ratio. Our studies thus show that the predominant crossover isomer is determined by the sequence at the junction, but they do not exclude the possibility that the sequence adjacent to the branching point may have an effect on the equilibrium distribution between the two crossover isomers.

The comparative analysis of our immobile HJs with the cruciform structure HJC16 (Pikkemaat *et al.*, 1994) sheds new light on the issue of the relevance of crossover isomer preference *in vivo*. Recent studies of a series of symmetric immobile junctions constructed from antiparallel double-crossover molecules (Fu & Seeman, 1993) suggest that the crossover isomer preferences in asymmetric immobile HJs may represent a maximum for a given base-pair arrangement (Zhang & Seeman, 1994). Using a system based on the sequence of J1, they found that the isomer preference was increasingly diluted by introducing increasingly larger segments of symmetry into the junction. It follows that in the context of the substantial sequence homology associated with homologous genetic recombination, crossover isomer preference may not be relevant. The comparison of these results on model HJs and those for HJC16 implies that conformational restriction at a distant site can induce molecular strain at the branching point. Thus, reservations due to possible strain in the double-crossover junctions (Zhang & Seeman, 1994) need to be carefully considered. The questions raised by our results provide strong motivation for further investigations into the sequence dependence of the structure, dynamics and crossover distribution of Holliday junctions, cruciforms, and related systems.

ACKNOWLEDGMENT

We thank Dr. James Fee and Dr. Pete Silks at the NIH Stable Isotope Resource for their efforts to produce the ^{15}N-labeled thymidine phosphoramidite, and Professor Ned Seeman, Professor Paul Hagerman, Dr. Shiow-Meei Chen,

and Dr. Siobhan Miick for their interest and helpful discussions.

SUPPORTING INFORMATION AVAILABLE

A summary of the sequential resonance assignment procedure for J2P1. Two figures with four panels each containing the $d_{i,s}$(1′H;6H,8H) and $d_{i,s}$(2′H,2″H;6H,8H) connectivities of J2P1 from 600 MHz JR-NOESY spectra, with cross-peaks labeled with sequence specific assignments for each strand in separate panels; one figure showing the complete list of assigned NOE connectivities involving the labile protons of J2P1 (12 pages). Ordering information is given on any current masthead page.

REFERENCES

Altona, C. (1990) in *Landolt-Börnstein. New Series* (Saenger, W., Ed.) Vol. 7/1c, pp 88−190, Springer-Verlag, Berlin.

Bodenhausen, G., Vold, R. L., & Vold, R. R. (1980) *J. Magn. Reson. 37*, 93−106.

Bodenhausen, G., Kogler, H., & Ernst, R. R. (1984) *J. Magn. Reson. 58*, 370−388.

Braunschweiler, L., & Ernst, R. R. (1983) *J. Magn. Reson. 53*, 521−528.

Braunschweiler, L., Bodenhausen, G., & Ernst, R. R. (1983) *Mol. Phys. 48*, 535−560.

Chen, S.-M., & Chazin, W. J. (1994) *Biochemistry 33*, 11453−11459.

Chen, S.-M., Heffron, F., & Chazin, W. J. (1993) *Biochemistry 32*, 319−326.

Chen, S.-M., Heffron, F., Leupin, W., & Chazin, W. J. (1991) *Biochemistry 30*, 766−771.

Cooper, J. P., & Hagerman, P. J. (1991) *Curr. Opin. Struct. Biol. 1*, 646−468.

Davis, D. G. (1989) *J. Magn. Reson. 81*, 603−607.

Drobny, G., Pines, A., Sinton, S., Weitekamp, D., & Wemmer, D. (1979) *Symp. Faraday Soc. 13*, 49−55.

Eis, P., & Millar, D. P. (1993) *Biochemistry 32*, 13852−13860.

Fu, T.-J., & Seeman, N. C. (1993) *Biochemistry 32*, 3211−3220.

Griffey, R. H., Poulter, C. D., Bax, A., Hawkins, B. L., Yamaizumi, Z., & Nishimura, S. (1983) *Proc. Natl. Acad. Sci. U.S.A. 80*, 5895−5897.

Hartel, A. J., Lankhorst, P. P., & Altona, C. (1982) *Eur. J. Biochem. 129*, 343−357.

Holliday, R. (1964) *Genet. Res. 5*, 282−304.

Jeener, J., Meier, B. H., Bachmann, P., & Ernst, R. R. (1979) *J. Chem. Phys. 71*, 4546−4553.

Kowalczykowski, S. C., Dixon, D. A., Eggleston, A. K., Lauder, S. D., & Rehrauer, W.M. (1994) *Microbiol. Rev. 58*, 401−465.

Lilley, D. M. J., & Clegg, R. M. (1993a) *Annu. Rev. Biomol. Struct. 22*, 299−328.

Lilley, D. M. J., & Clegg, R. M. (1993b) *Q. Rev. Biophys. 26*, 131−175.

Macke, T., Chen, S.-M., & Chazin, W. J. (1992) in *Structure and Function, 1, Nucleic Acids* (Sarma, R. H., & Sarma, M. H., Eds.) Vol. 1, pp 213−227, Adenine Press, Schenectady, NY.

Macura, S., & Ernst, R. R. (1980) *Mol. Phys. 41*, 95−117.

Marion, D., Ikura, M., Tschudin, R., & Bax, A. (1989) *J. Magn. Reson. 85*, 393−399.

Marky, L. A., Kallenbach, N. R., McDonough, K. A., & Seeman, N. C. (1987) *Biopolymers 26*, 1621−1634.

Mooren, M. M. W., Hilbers, C. W., van der Marel, G. A., van Boom, J. H., & Wijmenga, S. S. (1991) *J. Magn. Reson. 94*, 101−111.

Orbons, L. P. M., van der Marel, G. A., van Boom, J. H., & Altona, C. (1987) *Eur. J. Biochem. 170*, 225−239.

Oschkinat, H., Griesinger, C., Kraulis, P. J., Sørensen, O. W., Ernst, R. R., Gronenborn, A. M., & Clore, G. M. (1988) *Nature 332*, 374−376.

Oschkinat, H., Cieslar, C., Holak, T. A., Clore, G. M., & Gronenborn, A. M. (1989) *J. Magn. Reson. 83*, 450−472.

Otting, G., Senn, H., Wagner, G., & Wüthrich, K. (1986) *J. Magn. Reson. 70*, 500−505.

Pikkemaat, J. A., van den Elst, H., van Boom, J. H., & Altona, C. (1994) *Biochemistry 33*, 14896−14907.

Piotto, M. E., & Gorenstein, D. (1991) *J. Am. Chem. Soc. 113*, 1438−1440.

Plateau, P., & Guéron, M. J. (1982) *J. Am. Chem. Soc. 104*, 7310−7311.

Radhakrishnan, I., Patel, D., & Gao, X. (1991) *J. Am. Chem. Soc. 113*, 8542−8544.

Rance, M. (1987) *J. Magn. Reson. 74*, 557−564.

Rance, M., & Byrd, R. A. (1983) *J. Magn. Reson. 54*, 221−240.

Seeman, N. C. (1982) *J. Theor. Biol. 99*, 237−247.

Seeman, N. C., & Kallenbach, N. R. (1983) *Biophys. J. 44*, 201−209.

Seeman, N. C., & Kallenbach, N. R. (1994) *Annu. Rev. Biophys. Biomol. Struct. 23*, 53−86.

Shaka, A. J., Barker, P. B., & Freeman, R. (1985) *J. Magn. Reson. 64*, 547−552.

Shaka, A. J., Lee, C. J., & Pines, A. (1988) *J. Magn. Reson. 77*, 274−293.

Srinivasan, A. R., & Olson, W. K. (1994) *Biochemistry 33*, 9389−9404.

Stahl, F. W. (1994) *Genetics 238*, 241−246.

von Kitzing, E., Lilley, D. M. J., & Diekmann, S. (1990) *Nucleic Acids Res. 18*, 2671−2683.

Wemmer, D. E., Wand, A. J., Seeman, N. C., & Kallenbach, N. R. (1985) *Biochemistry 24*, 5745−5749.

Wüthrich, K. (1986) in *NMR of Proteins and Nucleic Acids*, John Wiley & Sons, New York.

Zhang, S., & Seeman, N. C. (1994) *J. Mol. Biol. 238*, 658−668.

BI952571N